

# Modeling and Analysis of Harmonic Resonance Involving Renewable Energy Sources

Jian Sun

**Abstract**— The resonance between power-factor-correction capacitors and the line reactance is a common cause for harmonic problems in traditional power systems. Grid-connected inverters integrating renewable energy sources into the grid exhibit capacitive output impedance at harmonic frequencies and may also resonate with the grid impedance. In addition to possible amplification of current and voltage harmonics, such resonances may lead to inverter control instability and other dynamic problems. This paper presents an overview of inverter modeling and system analysis methods for the characterization and mitigation of harmonic resonances involving renewable energy sources. The concept of sequence impedances is generalized to nonlinear circuits and used to model three-phase inverters at harmonic frequencies. A new harmonic resonance analysis method based on the Nyquist stability criterion is presented. Possible ways to shape the inverter output impedance to avoid resonances with the grid are highlighted, and the opportunity for adaptive inverter control based on real-time grid impedance measurement is discussed.

## I. INTRODUCTION

HARMONIC resonance is common in power systems. The resonance of line and transformer reactance with power-factor-correction (PFC) capacitors can lead to amplification of harmonic currents generated by nonlinear loads [1]. Other possible sources of harmonic resonance include underground cables and ferro-resonance of lightly loaded transformers [2]. With the increasing penetration of renewable energy in the power grid, inverters that interface with distributed generation (DG) resources such as solar and wind are becoming new potential sources of harmonics and harmonic resonance [3-9]. In addition to compliance issues with regulatory power quality standards [10], excessive harmonics and harmonic resonance may also lead to other problems such as damage of filter capacitors due to overheat, mechanical vibration of filter inductors, false trig of inverter and grid protection functions, as well as unintended shutdown of wind turbines and sometimes an entire wind farm.

Existing methods to model harmonics and harmonic resonance in solar [3-4] and wind power plants [5-9] follow the traditional power system harmonic analysis approach [11], in

which the inverter is modeled as a source of harmonic currents [3-5] or voltages [6, 7]. These harmonics are usually attributed to the inverter pulse-width modulation (PWM) control and are treated as harmonics of either the PWM carrier signal or the line fundamental [12, 13]. The carrier harmonics are normally well attenuated by inverter output filters and only become a concern for system harmonics when the switching frequency is low compared to the fundamental, such as in large wind and solar inverters where the switching frequency is limited to a few kHz or lower. Imperfect PWM control may result in low-order harmonics of the fundamental. Recently advances in circuit (such as multilevel converters) and PWM techniques provided many different ways to reduce or eliminate PWM-related harmonics. They also become less and less important as semiconductor power devices continue to improve and enable higher switching frequencies.

The network models used for system harmonic analyses in existing works include the impedance of the lines and cables, transformers, and filter components. The inverter is modeled as either a simple harmonic source, or a harmonic source with output impedance in the form of a Thevenin or Norton equivalent circuit. The report [7] by the IEEE PES Wind Plant Collector System Design Working Group pointed out the limitations of ideal harmonic source models and suggested the use of a Norton equivalent circuit model to account for the effects of inverter control on the output impedance and harmonic emission. However, existing inverter models cannot be used to support this type of analysis. As a result, existing system harmonic analysis either simply ignores inverter output impedance or considers only the impedance of passive filter components. Similar problems exist in harmonic and harmonic resonance analysis of other power systems involving voltage-source converters, see e.g. [14]. Ignoring control functions in the inverter model not only results in inaccurate and potentially incorrect harmonic predictions, but also misses the opportunity to mitigate harmonic problems through inverter control, which can be easier to implement and more cost effective.

This paper presents a new approach to the analysis and mitigation of power system harmonic and harmonic resonance problems involving renewable sources. The emphasis is on output impedance models of grid-connected inverters that can be used in system harmonic analysis. It is assumed that PWM carrier and other non-characteristic harmonics are small and can be ignored, such that an inverter can be adequately modeled by its output impedance for system harmonic analysis. A new method to detect potential resonances between the inverter output impedance and the grid impedance based on the Nyquist stability criterion is

---

This work was supported in part by the National Science Foundation under Award #ECCS-1002265 and by GE.

J. Sun is with the Department of Electrical, Computer, and Systems Engineering, Rensselaer Polytechnic Institute, Troy, NY 12180, USA (email: jsun@rpi.edu)

Paper submitted to the International Conference on Power Systems Transients (IPST2013) in Vancouver, Canada July 18-20, 2013.

presented. The concept of sequence impedances is generalized to nonlinear circuits and applied to three-phase inverters to develop output impedance models at harmonic frequencies. Possible ways to shape the output impedance through control of the inverter to avoid resonances with the grid are highlighted, and opportunities for adaptive inverter control based on real-time grid impedance measurement are discussed.

## II. INVERTER OUTPUT IMPEDANCE MODELING

Fig. 1 depicts an ideal three-phase two-level voltage-source converter as a basic building block for grid-connected inverters. For renewable energy applications, the dc bus is fed from solar panels or a wind turbine (through a rectifier), and the three ac terminals are connected to the grid, usually with additional filter capacitors to attenuate the PWM harmonics. An LCL filter configuration has also been proposed in the literature, see e.g. [15]. The following discussion will focus on inverters with simple inductive filtering. Additional filter components can be easily incorporated into the inverter model, or considered to be part of the grid impedance if they are not involved in the control of the inverter.

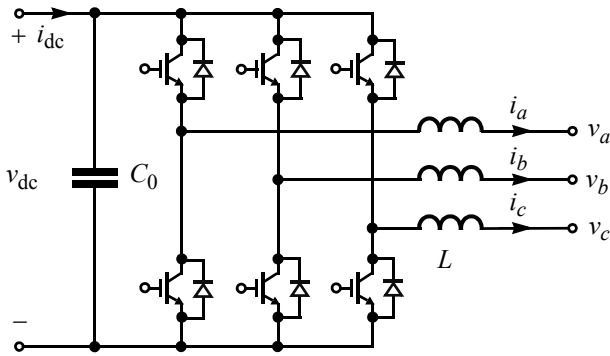


Fig. 1. Block diagram of three-phase voltage-source converter.

With reference to Fig. 1, the operation of a VSC can be described by the following equations where  $s_x$  is a binary function and represents the conduction state of phase  $x$  ( $= a, b, c$ ):  $s_x = 1$  when the upper-side switch conducts and  $-1$  when the lower-side switch conducts:

$$\begin{aligned} L \frac{di_a}{dt} &= s_a \frac{v_{dc}}{2} - v_a - v_N \\ L \frac{di_b}{dt} &= s_b \frac{v_{dc}}{2} - v_b - v_N \\ L \frac{di_c}{dt} &= s_c \frac{v_{dc}}{2} - v_c - v_N \\ C \frac{dv_{dc}}{dt} &= i_{dc} - [s_a i_a + s_b i_b + s_c i_c] \end{aligned} \quad (1)$$

Voltage  $v_N$  is the voltage of the ac (grid) neutral relative to the middle of the dc bus. This voltage consists of the common-mode components of the 2-level PWM phase voltages [16] and can be ignored in the modeling below the PWM carrier frequency, especially when there is no path for common-mode

currents<sup>†</sup>. For the same reason, the binary gate control signal of each phase leg can be replaced by its average over a carrier cycle using the duty ratio ( $d_x$ ) of the upper-side switch:

$$\begin{aligned} L \frac{di_a}{dt} &= \left(d_a - \frac{1}{2}\right) v_{dc} - v_a \\ L \frac{di_b}{dt} &= \left(d_b - \frac{1}{2}\right) v_{dc} - v_b \\ L \frac{di_c}{dt} &= \left(d_c - \frac{1}{2}\right) v_{dc} - v_c \\ C \frac{dv_{dc}}{dt} &= i_{dc} - [d_a i_a + d_b i_b + d_c i_c] \end{aligned} \quad (2)$$

The averaged model (2) is bilinear, as it involves the product between the control variables (duty ratios) and the state variables (dc bus capacitor voltage and ac phase inductor currents.) This nonlinearity is inherent in VSC and is one of the difficulties associated with their impedance modeling. However, since the dc bus capacitor is large and its dynamics are slow, the dc bus voltage can be treated as a constant when modeling the impedance above the grid fundamental frequency. The resulting *reduced-order model* is linear and independent of the circuit supplying the dc bus current,  $i_{dc}$ . This permits an output impedance model to be directly obtained when all controls are linear. For example, when each phase current is controlled by a PI controller as depicted in Fig.2, the output impedance of each phase is

$$Z_{in}(s) = \frac{Ls + V_{dc} K_m H_i(s)}{1 - V_{dc} K_m [H_i(s) G_r(s) + K_f(s)]} \quad (3)$$

where  $H_i(s)$  is the current compensator transfer function,  $K_m$  is the modulator gain, and  $K_f(s)$  is the grid voltage feedforward gain (see Fig. 2). The reference current,  $i_{ref}$ , is assumed to be proportional to the phase voltage by a gain  $G_r(s)$ . In the simplest case when a PI current compensator

$$H_i(s) = K_c \frac{1 + s/\omega_z}{s} \quad (4)$$

is used without grid voltage feedforward and the reference current is independent of the grid voltage,  $Z_{in}(s)$  simplifies to

$$Z_{in}(s) = Ls + V_{dc} K_m H_i(s). \quad (5)$$

Since the output impedance is identical for all three phases and uncoupled, the three-phase inverter can be represented by

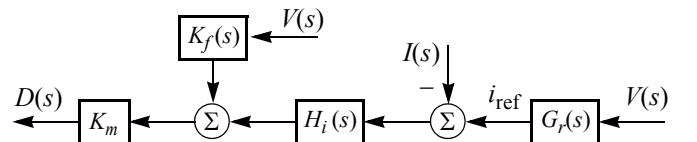


Fig. 2. Linear phase current control with grid voltage feedforward.

<sup>†</sup>. Common-mode currents cannot exist in a single inverter (except through parasitic elements), but may circulate among multiple inverters sharing the same dc bus and ac terminals.

a single-phase equivalent circuit consisting of a current source,  $I$ , in parallel with the output impedance,  $Z_{in}(s)$ , see Fig. 3. The use of a Norton instead of Thevenin equivalent circuit here is necessary because grid-connected inverters are usually controlled as current sources that cannot operate in an open-circuit configuration [17].

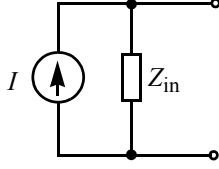


Fig. 3. Norton single-phase equivalent circuit representation of a three-phase inverter with independent linear phase current control.

Independent phase current control, however, is not very common in practice because of its limited performance. Most grid-connected inverters are controlled in a rotating (dq) reference frame synchronized to the grid voltage, and the synchronization is usually performed by a phase-locked loop (PLL) [18]. The PLL and the transformation to and from the dq domain introduce additional nonlinearity that cannot be avoided by the reduced-order modeling technique applied before, and the model must be linearized by other techniques in order to find the inverter output impedance.

The difficulty with linearizing a nonlinear inverter model is that there is no dc operation point to permit the application of conventional small-signal analysis methods. Traditional power system theories overcome this difficulty by using models expressed in terms of voltage and current phasors. Since both the amplitude and phase of a phasor are constant when the system enters steady-state, a nonlinear phasor model can be linearized by conventional small-signal methods. However, such phasor-based models are only valid at and below the line fundamental frequency and, hence, cannot be used in the analysis of harmonic resonance and other high-frequency phenomena related to grid-connected inverters. Additionally, a phasor model cannot be used to determine the input and output impedance of a converter [19].

A method to model three-phase converter impedance by harmonic linearization was developed in [20, 21] for line-commutated converters (LCC) and applied in [22] to three-phase VSC. In this method, a small-signal impedance model is obtained by directly calculating three-phase current responses to a small-signal harmonic perturbation in the three-phase voltages. Such current responses were found to depend on the sequence of the voltage perturbation for LCC as well as VSC with PLL-based control. Therefore, a voltage perturbation is further decomposed into positive, negative, and zero sequence components, as defined below.

1) Fundamental Voltage at  $f_1$

$$\begin{aligned} v_{a1} &= V_1 \cos(2\pi f_1 t) \\ v_{b1} &= V_1 \cos(2\pi f_1 t - 2\pi/3) \\ v_{c1} &= V_1 \cos(2\pi f_1 t - 4\pi/3) \end{aligned} \quad (6)$$

2) Positive-Sequence Perturbation at  $f_h$

$$\begin{aligned} v_{ap} &= \hat{V}_p \cos(2\pi f_h t + \phi_p) \\ v_{bp} &= \hat{V}_p \cos(2\pi f_h t + \phi_p - 2\pi/3) \\ v_{cp} &= \hat{V}_p \cos(2\pi f_h t + \phi_p - 4\pi/3) \end{aligned} \quad (7)$$

3) Negative-Sequence Perturbation at  $f_h$

$$\begin{aligned} v_{an} &= \hat{V}_n \cos(2\pi f_h t + \phi_n) \\ v_{bn} &= \hat{V}_n \cos(2\pi f_h t + \phi_n - 4\pi/3) \\ v_{cn} &= \hat{V}_n \cos(2\pi f_h t + \phi_n - 2\pi/3) \end{aligned} \quad (8)$$

4) Zero-Sequence Perturbation at  $f_h$

$$\begin{aligned} v_{a0} &= \hat{V}_0 \cos(2\pi f_h t + \phi_0) \\ v_{b0} &= \hat{V}_0 \cos(2\pi f_h t + \phi_0) \\ v_{c0} &= \hat{V}_0 \cos(2\pi f_h t + \phi_0) \end{aligned} \quad (9)$$

A zero-sequence perturbation produces no current, hence doesn't need to be considered. The current response to the positive-sequence and negative-sequence perturbation can each be calculated analytically based on the converter circuit and control by applying the harmonic linearization principle [20]. In general, the current response to a voltage perturbation in either sequence may contain both positive-sequence and negative-sequence components. This implies that the output admittance of a three-phase grid-connected inverter needs to be modeled in a matrix form as

$$\mathbf{Y}_{in} = \begin{bmatrix} Y_{pp} & Y_{pn} \\ Y_{np} & Y_{nn} \end{bmatrix} \quad (10)$$

where the off-diagonal terms represent cross-coupling between positive-sequence and negative-sequence components. However, it has been verified that, when the grid fundamental voltages are balanced, as in the case of (6), the negative-sequence current induced by a positive-sequence voltage perturbation and the positive-sequence current induced by a negative-sequence voltage perturbation are zero in the small-signal sense, that is, their magnitudes are high-order functions of the perturbation voltage. Because of that, the off-diagonal terms in (10) are zero and the inverter can be modeled by a positive-sequence output impedance,  $Z_p$ , and a negative-sequence output impedance,  $Z_n$ , without cross-coupling.

As an example, consider again the phase current control scheme depicted in Fig. 2. A PLL is used to synchronize the reference current with the grid voltage. The PLL, depicted in Fig. 4 uses dq transformation and a low-pass filter to extract the grid voltage phase angle ( $\theta_{pll}$ ) from the q-axis voltage [18]. Define the PLL loop gain as

$$T_{pll}(s) = \frac{V_1 H_{pll}(s)}{1 + V_1 H_{pll}(s)} \quad (11)$$

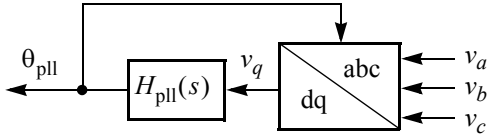


Fig. 4. Block diagram of a PLL based on dq transformation.

and denote the admittance of the inverter at the fundamental frequency as  $Y_1$ . The output impedances are found to be as follows when no grid voltage feedforward is used ( $K_f=0$ ) [22]:

$$Z_{ip}(s) = \frac{Ls + V_{dc}K_m H_i(s)}{1 - \frac{1}{2}T_{pll}(s - j2\pi f_1)V_{dc}K_m H_i(s)Y_1} \quad (12)$$

$$Z_{in}(s) = \frac{Ls + V_{dc}K_m H_i(s)}{1 - \frac{1}{2}T_{pll}(s + j2\pi f_1)V_{dc}K_m H_i(s)Y_1} \quad (13)$$

As an alternative to the harmonic linearization method, the three-phase averaged model (2) can be transformed to the dq reference frame. When the transformation is synchronized to the grid voltages, the phase voltages and currents become dc quantities in the dq coordinate system. The transformed model can, therefore, be linearized to calculate the inverter output impedance in the dq coordinate system. This method has been used to study the stability of three-phase PWM converters [23]. However, the resulting impedance model is not compatible with commonly used grid impedance models and are also difficult to measure or verify by experiments. Other limitations of this method have been discussed in [19].

### III. ANALYSIS OF HARMONIC RESONANCE

Harmonic resonance can be detected by scan of system impedance at harmonic injection points [2]. To locate the source of resonance, modal sensitivity analysis has been proposed [24] to determine how each resonant mode is related to different components of the system. Each of these methods has limitations when applied to renewable energy systems. A grid-connected inverter may emit harmonics due to PWM and imperfect control. However, the injection point of these harmonics is inside the inverter which is difficult to access for impedance scan. Besides, these harmonics are usually small and not a major concern for system harmonics. Modal analysis and other sensitivity analysis techniques require models of the entire network which renewable energy developers usually do not have access to.

An impedance-based stability analysis method was developed in [17] for single-phase grid-connected inverters. In this method, the inverter is represented by its Norton equivalent circuit (Fig. 3), and the grid is represented by an ideal voltage source in series with grid impedance, see Fig. 5. Based on this small-signal model, the grid current can be expressed as

$$I_g(s) = \frac{I(s)Z_{in}(s)}{Z_{in}(s) + Z_g(s)} - \frac{V_g(s)}{Z_{in}(s) + Z_g(s)} \quad (14)$$

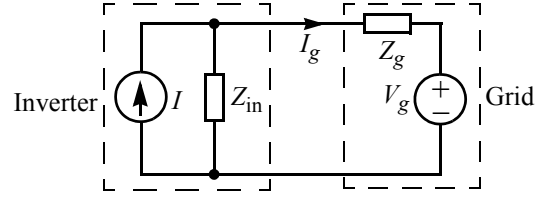


Fig. 5. Small-signal representation of an inverter-grid system.

which can be rearranged into

$$I_g(s) = \left[ I(s) - \frac{V_g(s)}{Z_{in}(s)} \right] \cdot \frac{1}{1 + Z_g(s)/Z_{in}(s)}. \quad (15)$$

Assuming that the inverter is properly designed and can operate with an ideal grid (zero impedance), (15) provides a mathematical model for the analysis of inverter control stability in the presence of grid impedance. Specifically, a grid-connected inverter will remain stable in the presence of grid impedance if the ratio of the grid impedance to the inverter output impedance,  $Z_g(s)/Z_{in}(s)$ , satisfies the Nyquist stability criterion [17].

In addition to inverter control stability analysis, the small-signal system model (15) can also be used to determine possible resonance between the inverter and the grid. Namely, an insufficient phase margin at frequencies where the inverter output impedance intersects with the grid impedance would indicate under-damped resonant modes. Such under-damped resonance can be periodically excited by switching and other nonlinearity of the inverter, leading to sustained harmonic currents at or near the resonant frequencies. The method has been successfully used to study harmonic resonance involving single-phase solar inverters [25].

This method can be directly applied to three-phase converters and systems that can be represented by a single-phase equivalent circuit, such as in the case when an inverter with linear phase current control (discussed at the beginning of Section II) is connected to a balanced grid. In more general cases, the inverter can be modeled by the admittance matrix (10) and the grid impedance can be represented by a similar sequence impedance matrix as [26]:

$$\mathbf{Z}_g = \begin{bmatrix} Z_{gp} & Z_{gpn} \\ Z_{gnp} & Z_{gn} \end{bmatrix} \quad (16)$$

It can then be seen that the interconnected inverter-grid system stability depends on the eigenvalues of

$$(\mathbf{I} + \mathbf{Y}_{in}\mathbf{Z}_g)^{-1} \quad (17)$$

where  $\mathbf{I}$  is a  $2 \times 2$  unity matrix. Therefore, the generalized Nyquist stability criterion [27] can be applied to the matrix  $\mathbf{Y}_{in}\mathbf{Z}_g$  to determine the stability and possible resonant modes.

The analysis is greatly simplified when the positive-sequence and negative-sequence responses are uncoupled. As discussed in the previous section, that is the case for typical grid-connected inverters. The grid impedance matrix also

degenerates into a diagonal form with no cross-coupling between positive and negative sequences when the grid is symmetrical. Therefore, a three-phase inverter connected to a balanced grid can be represented by a positive-sequence and a separate negative-sequence equivalent circuit as shown in Fig. 6. Since the two equivalent circuits are independent, Nyquist stability criterion can be applied separately to

$$\frac{Z_{gp}}{Z_{ip}} \quad \text{and} \quad \frac{Z_{gn}}{Z_{in}} \quad (18)$$

and the three-phase system is stable if and only if both sequence subsystems are stable. Similar to the single-phase case [17], lack of stability margin in either equivalent circuit implies harmonic resonance in the corresponding sequence.

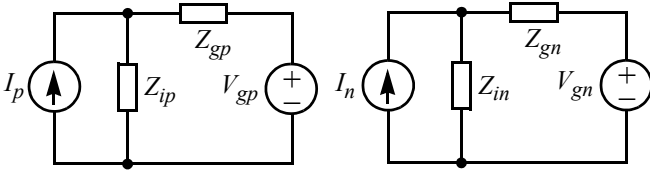


Fig. 6. Representation of a three-phase inverter connected to a balanced grid by independent positive-sequence and negative-sequence equivalent circuits.

The equivalent current sources in Fig. 6 model the inverter output current at the fundamental as well as harmonic frequencies when the grid is ideal, that is, a balanced grid without any impedance. Since such a grid does not exist in practice, these currents can be determined by detailed circuit simulation or measurement with a strong grid if possible. For the purpose of harmonic resonance analysis based on the Nyquist stability criterion, these current sources do not matter and both can be treated as open-circuits.

Similarly, the equivalent voltage sources in Fig. 6 represent the fundamental as well as harmonic components of the grid voltage. Hence the equivalent circuits can also be used to study the effects of source unbalance and background harmonic distortion on system harmonic currents. For a harmonic-free, balanced three-phase grid, all voltages except the positive-sequence fundamental voltage are zero. Additionally,  $Z_{gp} = Z_{gn}$  if the grid contains only passive elements [26].

The inverter output impedances become coupled when the grid voltages are unbalanced. However, the off-diagonal terms in the impedance matrix are found to be proportional to the level of voltage unbalance measured in per-unit values. Therefore, the off-diagonal terms are at least 20 dB lower than the diagonal terms for a normal unbalanced grid where the unbalance is typically less than a few percent. Considering that, the separate equivalent circuits in Fig. 6 can be used for practical purposes unless there is a asymmetrical fault in the system that causes severe voltage unbalance.

#### IV. APPLICATIONS

This section presents laboratory test results to demonstrate the application of the proposed impedance modeling and harmonic resonance analysis methods. The experimental setup is illustrated in Fig. 7 and consists of a three-phase inverter rated at 20 kW as well as a grid simulator [25, 28]. The grid simulator was developed to provide a controllable grid with programmable voltage, frequency, harmonic contents, as well as impedance. It consists of an active part built using back-to-back VSC and a passive part using adjustable inductors and capacitors.

The inverter was built in-house and employs a DSP and an FPGA control board. Its control structure is illustrated in Fig. 7 and consists mainly of three parts: a) a PLL for synchronization with the grid voltage, b) dq-domain current control, and c) pulse-width modulation. In all experiments presented here, the inverter was fed from a programmable dc power source and the dynamics of the dc bus are not considered. A 3.6 mH inductor ( $L$ ) is placed at each ac phase terminal. Three star-connected capacitors (each 22  $\mu$ F) are used to provide additional filtering of PWM harmonics. Each capacitor is also connected in series with a 1.87  $\Omega$  to provide damping. However, to simplify the inverter impedance models, these capacitors and resistors are lumped with the grid (as indicated in Fig. 7) and are included in the grid impedance model. The DSP and FPGA control boards sample the grid voltages and currents at 50  $\mu$ s and 25  $\mu$ s intervals, respectively, and the corresponding sampling effects are included in the inverter impedance models. Fig. 8 shows the responses of the inverter output impedances  $Z_{ip}$  and  $Z_{in}$  as defined in the previous section. The dots represent the responses measured by a frequency analyzer for comparison.

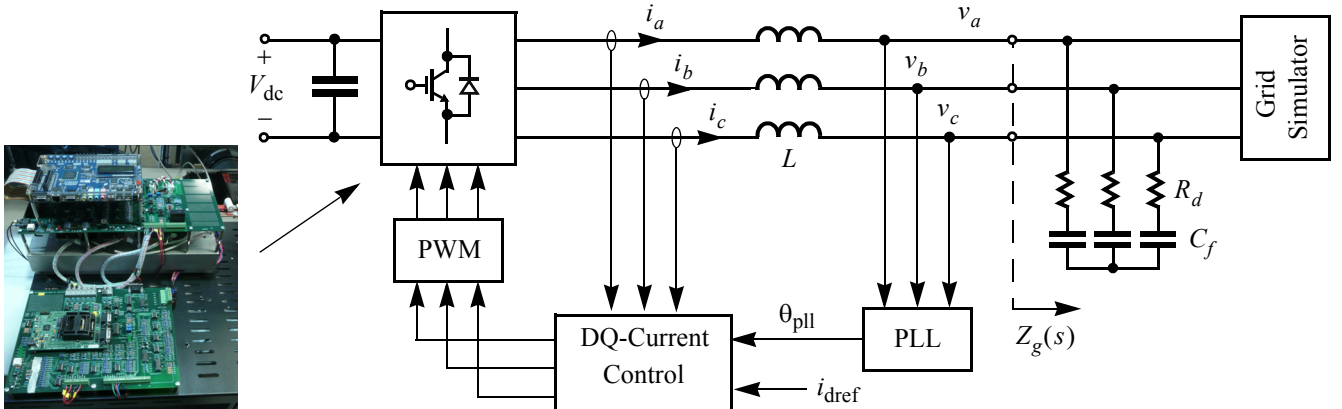


Fig. 7. Experimental setup for testing a three-phase inverter connected to a balanced grid with variable grid inductance.

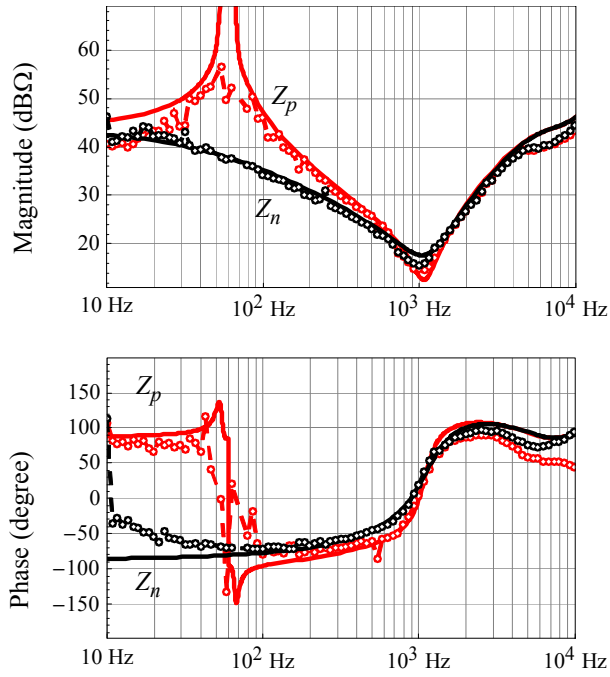


Fig. 8. Positive-sequence and negative-sequence output impedance responses of a three-phase inverter. Solid lines: model predictions; Dash-dot: experimental measurements.

As can be seen from Fig. 8, both the positive-sequence and negative-sequence impedances are capacitive above the grid fundamental frequency. The phase of the positive-sequence impedance even exceeds  $-90^\circ$  around 100 Hz. Since the grid impedance is inductive, with close to  $+90^\circ$  phase angle in this frequency range, a resonance will be formed if the two impedances intersect with each other in this frequency range, and such a resonance would be very lightly damped or even unstable because of the close to  $180^\circ$  phase difference between the inverter and grid impedance. Based on Fig. 8, the resonance is more likely to occur with the positive-sequence impedance because of its larger phase shift.

Fig. 9 shows two sets of inverter output current measurements and their harmonic contents obtained by Fourier analysis. In the first case, the bandwidth of the PLL used to synchronize with the grid was set at 100 Hz, and the corresponding current responses of the inverter are shown in Fig. 9a). Large distortion due to harmonic resonance between the inverter and the grid can be seen. Fig. 9c) shows the spectrum of the inverter output current and the Nyquist plot of the ratio of the grid impedance to the inverter output impedance. The positive-sequence impedance ratio shows that the system is stable but with less than  $20^\circ$  phase margin around 200 Hz. The small phase margin leads to an under-damped resonance and explains the observed strong 3<sup>rd</sup> and 4<sup>th</sup> harmonics.

Fig. 9b) shows the measured current waveforms when the PLL bandwidth was reduced to 10 Hz. The corresponding current spectrum and Nyquist plots of the impedance ratio are shown in Fig. 9c) as well for comparison with the first case. As can be seen, both the positive- and the negative-sequence impedance ratio has sufficient phase margin in this case, which effectively eliminated the harmonic resonance.

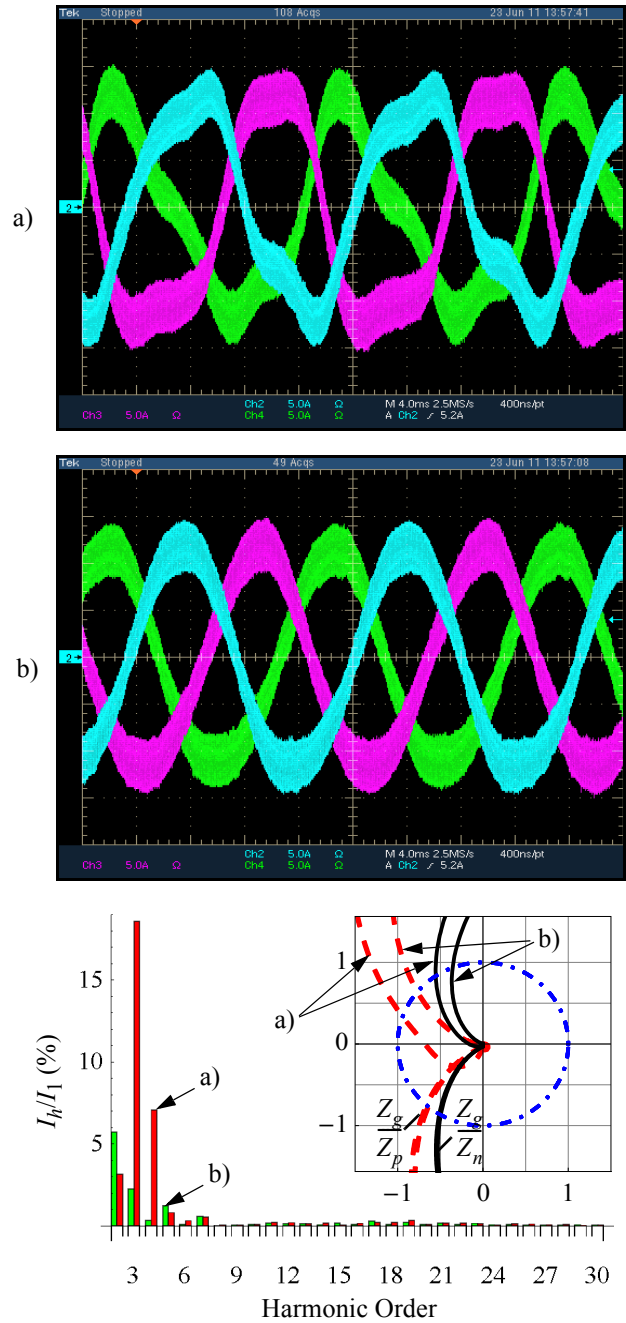


Fig. 9. Mitigation of harmonic resonance in the experimental system by reduction of PLL bandwidth: a) 100 Hz PLL bandwidth; b) 10 Hz PLL bandwidth.

These measurements demonstrated the importance of both inverter control and grid impedance in harmonic performance of grid-connected inverters. To reduce the risk for resonance, the inverter output impedance should be as high as possible, ideally above the grid impedance at all frequencies. Since this is impractical due to the inductive nature of grid impedance, it is important to identify the frequencies at which the inverter and the grid impedance intersect, and to ensure sufficient phase margin through proper inverter control design [29]. The analytical impedance models provide a means for such design. Additionally, since the grid impedance changes from site to site and may vary over time, adaptive control based on real-time grid impedance measurement may be considered [30].

## V. CONCLUSIONS

Although PWM switching ripple and non-characteristic harmonics caused by imperfect control of grid-connected inverters may contribute to grid system harmonics, resonance between the inverter output impedance and the grid impedance is a more likely source of harmonics in renewable energy systems. The combination of harmonic linearization and sequence impedance decomposition provides an effective and systematic method to model inverter output impedance for system harmonic resonance analysis. Under balanced or mildly unbalanced grid conditions, a three-phase inverter-grid system can be decomposed into a positive-sequence and a negative-sequence subsystem, and Nyquist stability criterion can be applied to each subsystem separately to determine system stability as well as possible resonant modes.

A marginally stable inverter current control loop in the presence of high grid impedance is a common source of system harmonic resonance. To ensure stable operation under different grid conditions, a grid-connected inverter should be designed to have as high output impedance as possible. The analytical impedance models presented in this paper also provide a means to shape the inverter output impedance through control and circuit design of grid-connected inverters to avoid undamped resonances. Adaptive control such as gain scheduling can be used in conjunction with online grid impedance identification techniques to guarantee stable and harmonic-free operation under variable grid conditions.

## REFERENCES

- [1] G. Lemieux, "Power system harmonic resonance: a documented case," in *Record of IEEE 1988 Annual Pulp and Paper Industry Technical Conference*, pp. 38-42, 1988.
- [2] R. C. Dugan, M. F. McGranaghan, S. Santoso, and H. W. Beaty, *Electrical Power Systems Quality*, McGraw-Hill, 2nd Ed., 2002.
- [3] J. H. R. Enslin and P. J. M. Heskes, "Harmonic interaction between a large number of distributed power inverters and the distribution network," *IEEE Transactions on Power Electronics*, vol. 19, no. 6, pp. 1586-1593, 2004.
- [4] A. Bhowmik, A. Maritra, S. M. Halpin, and J. E. Schatz, "Determination of allowable penetration levels of distributed generation resources based on harmonic limit considerations," *IEEE Transactions on Power Delivery*, vol. 18, no. 2, pp. 619-624, 2003.
- [5] J. Li, N. Samaan, and S. Williams, "Modeling of large wind farm systems for dynamic and harmonic analysis," in *Proc. of 2008 IEEE Transmission and Distribution Conference and Exhibition*, pp. 1-7, 2008.
- [6] R. King and J. B. Ekanayaka, "Harmonic modeling of offshore wind farms," in *Proc. 2010 IEEE Power and Energy Society General Meeting*, pp. 1-6, July 2010.
- [7] M. Bradt, B. Badrzadeh, E. Camm, D. Mueller, J. Schoene, T. Siebert, T. Smith, M. Starke, and R. Walling, "Harmonics and resonance issues in wind power plants," in *Proc. 2012 IEEE Power and Energy Society General Meeting*, pp. 1-8, July 2012.
- [8] K. N. M. Hasan, K. Rauma, P. Rodriguez, J. I. Candela, R. S. Munoz-Aguilar, and A. Luna, "An overview of harmonic analysis and resonances of large wind power plant," in *Proc. IECON 2011 - 37th Annual Conference of IEEE Industrial Electronics Society*, pp. 2467-2474, 2011.
- [9] K. N. M. Hasan, K. Rauma, A. Luna, J. I. Candela, P. Rodriguez, "Harmonic resonance damping in wind power plant," in *Proc. IEEE 2012 Energy Conversion Congress and Exposition (ECCE)*, pp. 2067-2074, September 2012.
- [10] IEEE Application Guide for IEEE Std 1547™, IEEE Standard for Interconnecting Distributed Resources with Electric Power Systems, IEEE Standards Coordinating Committee 21, April 2009.
- [11] J. Arrillaga, B. C. Smith, N. R. Watson, A. R. Wood, *Power System Harmonic Analysis*, John Wiley & Sons, Ltd, 1997.
- [12] B. Badrzadeh, M. Gupta, N. Singh, A. Petersson, L. Max, and M. Hogdahl, "Power system harmonic analysis in wind power plants - part I: study methodology and techniques," in *Proc. IEEE Industry Applications Society 2012 Annual Conference*, pp. 1-8, 2012.
- [13] B. Badrzadeh and M. Gupta, "Power system harmonic analysis in wind power plants - part II: experiences and mitigation methods," in *Proc. IEEE Industry Applications Society 2012 Annual Conference*, pp. 1-8, 2012.
- [14] K. Temma, F. Ishiguro, N. Toki, I. Iyoda, and J. J. Paserba, "Clarification and measurements of high frequency harmonic resonance by a voltage sourced converter," *IEEE Transactions on Power Delivery*, vol. 20, no. 1, pp. 450-457, January 2005.
- [15] E. Twining and D. G. Holmes, "Grid current regulation of a three-phase voltage source inverter with an LCL input filter," *IEEE Transactions on Power Electronics*, vol. 18, no. 3, pp. 888-895, May 2003.
- [16] T. Qi and J. Sun, "Analysis and reduction of common-mode EMI in electric actuators for VF MEA," in *Proceedings of SAE 2010 Power Systems Conference*, CD-ROM, Paper # 2010-01-1740, November 2010.
- [17] J. Sun, "Impedance-based stability criterion for grid-connected inverters," *IEEE Transactions on Power Electronics*, vol. 27, no. 11, Nov. 2011.
- [18] R. Teodorescu, M. Liserre, and P. Rodriguez, *Grid Converters for Photovoltaic and Wind Power Systems*, Wiley-IEEE, 2011.
- [19] J. Sun, "Small-signal methods for ac distributed power systems," *IEEE Transactions on Power Electronics*, vol. 24, no. 11, pp. 2545-2554, November 2009.
- [20] J. Sun, Z. Bing, and K. Karimi, "Input impedance modeling of multipulse rectifiers by harmonic linearization," *IEEE Transactions on Power Electronics*, vol. 24, no. 12, pp. 2812-2820, December 2009.
- [21] Z. Bing and J. Sun, "Frequency-domain modeling of multipulse converters by double-Fourier series method," *IEEE Transactions on Power Electronics*, vol. 27, no. 11, 3804-3809, Dec. 2011.
- [22] M. Cespedes and J. Sun, "Impedance modeling and analysis of grid-connected three-phase voltage-source converters," to appear in *IEEE Transactions on Power Electronics*.
- [23] M. Belkhaty, "Stability Criteria for AC Power Systems with Regulated Loads," PhD dissertation, Purdue University, 1997.
- [24] Z. Huang, Y. Cui, and W. Xu, "Application of modal sensitivity for power system harmonic resonance analysis," *IEEE Transactions on Power Systems*, vol. 22, no. 1, pp. 222-231, February 2007.
- [25] X. Chen and J. Sun, "A study of renewable energy system harmonic resonance based on a DG test-bed," in *Proc. IEEE 2011 Applied Power Electronics Conference*, pp. 995-1002, Ft. Worth, TX, March 2011.
- [26] E. Clarke, *Circuit Analysis of A-C Power Systems*, General Electric Co., Schenectady, NY, 1950.
- [27] A. G. J. MacFarlane, *Complex Variable Methods for Linear Multivariable Feedback Systems*, Taylor and Francis Ltd., 1980.
- [28] M. Cespedes, T. Qi and J. Sun, "Development of a grid simulator," in *Proc. IEEE 2012 Workshop on Control and Modeling for Power Electronics (COMPEL 2012)*, June 2012.
- [29] M. Cespedes and J. Sun, "Impedance shaping of three-phase grid-parallel voltage-source converters," in *Proc. IEEE 2012 Applied Power Electronics Conference*, pp. 754-760, February 2012.
- [30] M. Cespedes and J. Sun, "Online identification of grid impedance for adaptive control of grid-connected inverters," in *Proc. IEEE 2012 Energy Conversion Congress and Exposition (ECCE 2012)*, pp. 914-921, Raleigh, North Carolina, September 2012.